Lava loads superposed on Martian glaciers: An assessment of ice-flow velocity enhancements

J. L. FASTOOK[1], J. W. HEAD[2]

1-University of Maine, 2-Brown University

Introduction:

Evidence exists for a "wet/warm" early Mars **[1]** (fluvial landforms such as valley networks **[2-6]**, open- and closed-basin lakes **[7-9]**, and evidence for phyllosilicates [10-11]), but such a climate is difficult to reproduce with climate models **[12-14]**. An alternative hypothesis, the "icy-highlands" model, proposes that water ice, preferentially deposited in an adiabatic atmosphere at higher elevations, serves as a reservoir for the release of liquid water to create the observed features [13-14]. One mechanism to release liquid water from the icy-highlands reservoirs is the increased volcanism that occurred in the late Noachian and early Hesperian **[15-17]**. Cassanelli and Head **[18,19]** have quantified the amount of liquid water that would be released from regional ice sheets of different thicknesses for different thicknesses of superposed lava and related that water release to various landforms indicative of liquid water.

We focus on the impact of superposed lava on the flow characteristics of the ice, assessing the following:

1) How the **added overburden** of the superposed lava affects the flow through the **increased driving stress**
2) How the competing effect of **thinning ice due to top-down melting** affects the flow through the **decreasing driving stress**
3) How the **top-down melting** of the ice affects its **internal temperature distribution** and consequent **ice hardness** through the Arrheniusly-activated Flow Law.

Modeling:

We employ a 1D time-dependent heat-flow solver based on the University of Maine Ice Sheet Model **[20, 21]**, run as a coupled model for the superposed lava layer and the underlying ice, with boundary conditions matched at the lava-ice interface.

This Finite-Element Model incorporates explicit formulations for both Dirichlet and Neumann boundary conditions, so that given a specified boundary temperature, one can solve for the required flux necessary to hold that boundary at the required temperature. This required flux at the lava-ice interface, derived from the latent heat of fusion of ice, allows us to calculate the amount of ice melted as the lava layer cools. Using the same material properties and initial temperature distribution as Cassanelli and Head **[18,19]** we obtain the same 4.5:1 ratio of melted ice to lava thickness that they obtained using a completely different heat flow solution.

The lava boundary conditions are initially 225 K at the surface and 273 K at the base with an initial uniform 1350 K for the interior. As the temperature profile relaxes with time, melting at the base is calculated until the profile reaches equilibrium for a geothermal heat flux of 50 mW/m^2, at which point the lava-ice interface boundary condition is switched to a Neumann flux boundary condition and the base continues to cool until it equilibrates with a temperature gradient of 26.45 K/km typical of the prescribed heat flux.

The time-dependent lava-ice interface temperature provides the ice-surface boundary condition for the coupled ice temperature model, again with the basal boundary condition being the specified geothermal flux. We also allow for the possibility of basal melting if the ice bed ever reaches the melting point and can calculate the amount of ice melted there.

The thinning rate due to top-down melting produced by the lava model, which starts high and declines exponentially, is used in the ice model to progressively thin the ice, done by regridding interpolated temperatures during each time step.

We run the ice model for 10 Ka with 225 or 245 K surface temperatures to insure equilibrium. At that point we switch the surface boundary condition to the melting point for the duration of the lava-induced melting event. Following the melting event the surface temperature is prescribed by the lava model's lava-ice interface temperature as the lava cools to its equilibrium profile.

Results:

The interplay of these effects produces interesting results. The rapid transition from 225 or 245 K at the ice surface to 273 K sends a wave of heat into the ice column that manifests at the base of the ice as delayed warming, analogous to the "deferred warming" described by [18,19].

The time for a change in surface temperature to reach the bed is shown in **Figure 1**. This relaxation time for reduction to 1/e of the temperature difference ranges from 100 years for 100 m ice to almost 10,000 years for 1000 m ice.

The temperature at the top surface of the ice, specified by the bottom temperature of the lava that has dropped below 273 K, then gradually cools to a temperature slightly warmer than the initial 225 or 245 K due to the insulating lava, but the thinning ice provides less insulation to the bed, so the basal temperature will actually cool.

One such basal temperature as a function of time is shown in **Figure 2** for 500 m ice with a 90 m lava layer with an initial surface temperature of 225 K. With the event beginning at 10 Ka, we can see a lag of approximately 100 years before the basal temperatures begin to increase, even though the warming event itself only lasts 170 years (from **Table 1**).

This warming of the bed is also summarized in **Table 1** showing results for two surface temperatures, 225 and 245 K Ice melting ranges from 45 m for a 10 m lava layer to 928 m for a 200 m lava layer. The difference between the two cases results from the differences in the upward and downward fluxes of heat from the lava, with slightly more heat conducted downward for the warmer surface.

Also shown are the durations of the various melting events, ranging from 2 years for 10 m of lava to 929 for 200 m. Also shown is the bottom warming as the lava relaxes to equilibrium, which is used in the ice model as the top boundary condition once the melting event is over. In general warming increases with lava thickness and decreases with ice thickness, with lesser amplitudes for the warmer 245 K surface temperature.

Analysis:

Our guiding question has been **how the superposed lava will influence the flow**, and we are dealing with three competing effects:

1) **The added driving stress due to the weight of the lava,**
2) **The softer ice during the transient warming of the ice column, and**
3) **The reduced driving stress due to the thinning of the ice column by the top-down melting.**

Velocity is obtained by integrating the strain rates from the bed to the surface, accounting for the temperature-dependent ice hardness and the n=3 exponent in the Flow Law. We choose a slope of 1 degree to calculate velocities, but any other slope would simply scale as the slope cubed.

An example of the behavior observed is shown in **Figure 1** for 500 m ice with 90 m lava and a surface temperature of 225 K. We see two peaks: the initial peak due to the increased driving stress from the instantaneous loading of 90 m of lava onto the ice surface. This peak, which accelerates flow by a factor of 5.23, is short-lived, 29 years.

The results for the primary and secondary peaks for different ice and lava thicknesses are summarized in **Table 2**. While the primary peak always shows some acceleration, ranging from a few percent to factors of 5 or more, the secondary peak only shows acceleration for the largest lava thicknesses that in fact have melted away almost the entire ice thickness.

In the acceleration column of the secondary peak, a second acceleration is shown that is the increase from the minimum reached before the second peak starts. Of further note is the duration of the secondary peak, which in general is much longer for thicker ice and displays a maximum, usually in the mid range of lava thicknesses examined

Lava Thickness (m) for 225 / 245K	Ice Thickness Melted (m)	Duration of Melting (yr)	Lava Base Warming	Temperature Warming (K) Ice Thickness (m) 100	500	1000
10	45.86 / 46.43	2.09 / 2.34	0.26	2.54 / 1.37	0.06 / 0.02	0.16 / 0.053
20	91.66 / 92.82	8.50 / 9.50	0.53	41.05 / 24.58	0.21 /0.07	0.17 / 0.057
30	137.58 / 139.29	18.8 / 21.1	0.79	----	0.62 / 0.25	0.20 / 0.064
40	183.27 / 185.61	34.0 / 38.0	1.06	----	1.49 /0.64	0.28 / 0.086
50	229.20 / 232.09	52.5 / 59.0	1.32	----	3.10 / 1.42	0.42 / 0.13
60	274.94 / 278.45	76.0 / 85.0	1.59	----	5.89 / 2.81	0.63 / 0.20
70	320.87 / 324.93	103 / 116	1.85	----	10.35 / 5.10	0.95 / 0.31
80	366.79 / 371.40	135 / 150	2.12	----	17.23 / 8.74	1.40 / 0.48
90	412.70 / 417.86	170 / 190	2.38	----	27.31 / 14.12	2.03 / 0.71
100	458.61 / 464.33	209 / 234	2.65	----	38.74 / 18.11	2.87 / 1.04
125	573.34 / 580.47	326 / 364	3.31	----	----	6.23 / 2.35
150	688.09 / 696.60	469 / 524	3.97	----	----	12.20 / 4.68
175	802.82 / 812.73	637 / 712	4.63	----	----	21.99 / 8.29
200	917.54 / 928.86	832 / 929	5.29	----	----	30.79 / 8.29

Table 1: Results from the lava temperature model relaxing from 1350K to an equilibrium profile for various lava layer thicknesses. Basal warming for various lava and ice thicknesses for 225 and 245 K

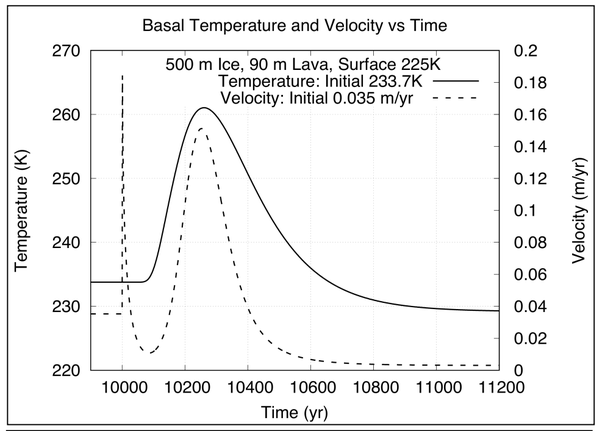

Figure 2: Basal Temperatures and Velocities for 500 m Ice, 90 m Lava with Surface Temperature 225K.

225 K Lava (m)	Peak 1 MaxV	Accelerat	Duration	Peak 2 MaxV	Accelerat	Duration
100 m Ice Base Velocity 2.75 X 10^{-5}						
10	7.6 X 10^{-5}	2.8	0.30	1.2 X 10^{-5}	0.45/1.35	74
20	1.7 X 10^{-4}	6.1	1.00	7.8 X 10^{-5}	2.85/47.9	15
500 m Ice Base Velocity 0.035						
10	0.044	1.26	0.41	0.031	0.89/1.00	454
20	0.055	1.56	1.7	0.028	0.80/1.02	641
30	0.068	1.92	3.6	0.026	0.74/1.07	741
40	0.082	2.32	7	0.025	0.71/1.19	787
50	0.098	2.78	10	0.026	0.74/1.42	769
60	0.12	3.29	15	0.031	0.86/1.92	709
70	0.14	3.87	19	0.042	1.20/3.05	624
80	0.16	4.52	24	0.072	2.05/5.95	536
90	0.18	5.23	29	0.15	4.29/14.0	441
100	0.21	6.02	34	0.47	13.23/49.	317
1000 m Ice Base Velocity 1.36						
10	1.55	1.12	0.41	1.31	0.95/1.00	1135
20	1.73	1.25	1.8	1.24	0.90/1.00	1311
30	1.93	1.39	3.8	1.18	0.85/1.01	1511
40	2.14	1.55	7.5	1.12	0.81/1.02	1765
50	2.36	1.71	11	1.07	0.77/1.03	1847
60	2.60	1.88	16	1.03	0.74/1.06	2043
70	2.86	2.07	21	1.00	0.72/1.10	2100
80	3.14	2.27	27	0.99	0.71/1.16	2140
90	3.43	2.48	33	0.98	0.72/1.24	2142
100	3.74	2.70	40	1.01	0.73/1.36	2134
125	4.60	3.32	60	1.23	0.89/1.93	2011
150	5.58	4.04	83	1.93	1.39/3.47	1813
175	6.69	4.84	109	4.39	3.18/8.70	1544
200	7.95	5.75	136	15.2	10.97/31.	1172

Table 2: Primary and secondary peak velocities, accelerations, and durations for various ice and lava thicknesses

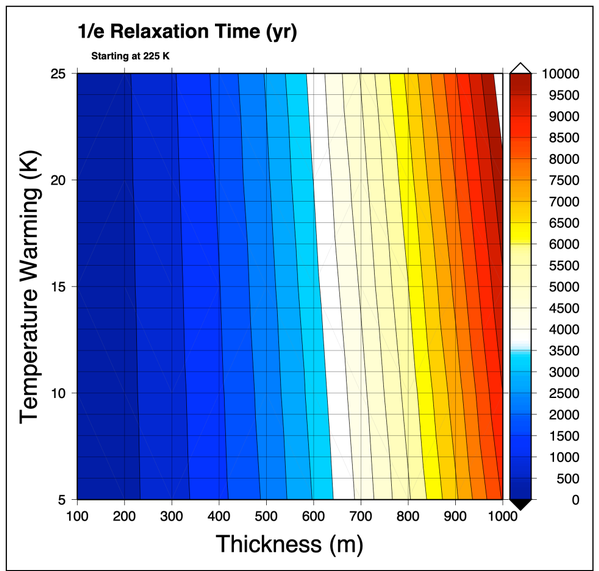

Figure 0: The relaxation time to 1/e of the initial temperature at the bed for various ice thicknesses and amounts of surface warming

Conclusions:

The interplay of competing effects provides some insight into the response of the flow of ice to a lava layer being deposited on its surface.

- **Melt amounts agree with the Cassanelli and Head [18,19] estimates based on a completely different numerical scheme.**
- **The primary acceleration peak appears to be due to the added overburden of the deposited lava through the increased driving stress but is generally short-lived as the ice rapidly thins due to top-down melting.**
- **A secondary acceleration produced by the thermal wave reaching the bed is only able to accelerate the ice above its pre-deposition velocity for the largest lava thicknesses that remove at least 40% of the initial ice thickness, but the duration of these peaks is orders of magnitude longer.**
- **Only in the most extreme cases where 90% of the initial ice thickness was removed by top-down melting (100 m lava for to 500 m ice and 200 m for the 1000 m ice case) did the bed approach or exceed the melting point, and when it did the basal melting was brief and produced little water (0.4 m over 50 years for 100 m lava on 500 m ice and 2.4 m for 200 m lava on 1000 m ice, both with a warmer surface temperature of 245 K)**

[1] Craddock R. A. and Howard A. D. (2002) *JGR*, *107*, 21–36. [2] Howard A. D. (2007) Geomorphology, 91, 332–363. [3] Fassett C. I. and Head J. W. (2008) *Icarus*, *195*, 61–89. [4] Barnhart C. J. et al. (2009) *JGR*, *114*, E01003.]5] Hynek B. M. et al. (2010) *JGR*, *115*, E09008. [6] Hoke M. R. T. et al. (2011) *Earth Planet. Sci. Lett.*, *312*, 1–12. [7] Cabrol N. A. and Grin E. A. (1999) *Icarus*, *142*, 160–172. [8] Carr M. H. (2007) The Surface of Mars. Cambridge University Press, UK. [9] Fassett C. I. and Head J. W. (2008) *Icarus*, *198*, 37–56. [10] Bibring J.-P. et al. (2006) *Science*, *312*, 400–404. [11] Ehlmann et al. (2011) *Nature*, *479*, 53–60. [12] Forget F. et al. (2013) *Icarus*, *222*, 81–99. [13] Wordsworth R. et al. (2013) *Icarus*, *222*, 1–19. [14] Wordsworth R. et al. (2015) *JGR Planets*, *120*, 1201–1219. [15] Craddock R. A. and Greeley R. (2009) *Icarus*, *204*, 512–526. [16] Rogers A. D. and Nazarian A. H. (2013) *JGR Planets*, *118*, 1094–1113. [17] Tanaka K. L. et al. (2014) *Planet. Space Sci.*, *95*, 11–24. [18] Cassanelli P. and Head J. W. (2016) *Icarus*, *271*, 237–264. [19] Cassanelli P. and Head J. W. (2018) *Planetary and Space Science*, 158, 96-109. [20] Becker E. B. et al. (1981) Finite Elements, An Introduction. Prentice-Hall, Englewood Cliffs. [21]